

Supplementary Material

Low-concentration cholesterol modification enhances *Clematis filamentos*a Dunn-derived extracellular vesicle-mediated macrophage polarization regulation for acute lung injury therapy

Guanglin Zhang^{1,2*}, Huadong Liang^{2*}, Guanyan Zhang³, Changyao Chen², Junjie Lai², Hongjia Huang⁴, Liubing Hu⁴, Baiyin Yu^{1,2}, Xiang Li^{1,2}, Rong Zeng³, Jie Chen^{1,2}

¹ Guangdong Province Key Laboratory of Utilization and Conservation of Food and Medicinal Resources in Northern Region, Shaoguan University, Shaoguan, Guangdong 512005, P. R. China

² College of Biology and Agriculture, Shaoguan University, Shaoguan, 512005, P. R. China

³ Department of Materials Science and Engineering, College of Chemistry and Materials, Jinan University, Guangzhou, 510632, P. R. China

⁴ College of Life Science and Technology, Jinan University, Guangzhou, 510632, P. R. China

Correspondence: Jie Chen, College of Biology and Agriculture, Shaoguan University, Shaoguan, 512005, P. R. China, Email maggiecj049@sgu.edu.cn.

*: Guanglin Zhang and Huadong Liang contributed equally to this work.

1. Materials and Methods

1.1 RAW264.7 cell culture

RAW264.7 cells (purchased from ATCC) were cultured in Dulbecco's Modified Eagle Medium (DMEM) supplemented with 10% (v/v) fetal bovine serum and maintained at 37° C in a humidified atmosphere containing 5% CO₂. For M1 macrophages polarization, cells were stimulated with 100 ng/mL lipopolysaccharide (LPS) for 12 h. For M2 macrophages polarization, cells were treated with a combination of 20 ng/mL interleukin-4 (IL-4) and 20 ng/mL interleukin-13 (IL-13) for 12 h.

1.2 Isolation of *Clematis filamento*s Dunn-derived nanovesicles (CDNVs)

Fresh levels of *Clematis filamento*s Dunn were thoroughly rinsed with phosphate-buffered saline (PBS), manually minced, and homogenized in ice-cold PBS using a high-throughput tissue disruptor. The resulting homogenate was sequentially filtered through a 100-mesh nylon sieve and subjected to centrifugation at $4,000 \times g$ for 30 min at 4°C to remove large particulate debris. The supernatant was then further clarified by centrifugation at $10,000 \times g$ for 1 h at 4°C to eliminate cellular debris, followed by filtration through a $0.8 \mu\text{m}$ polyethersulfone (PES) membrane to obtain clear plant sap. Three distinct isolation methods—ultrafiltration, sucrose density gradient ultracentrifugation, and polyethylene glycol (PEG) precipitation—were systematically optimized as described below:

1.2.1 Ultrafiltration-based isolation (CDNVs1)

The clarified plant sap was loaded into an Amicon® Ultra-15 centrifugal filter unit with a 100 kDa molecular weight cutoff (Merck, Millipore) and centrifuged at $5,000 \times g$ for 1 h at 4°C . The retained fraction was collected and subjected to five successive extrusions through a 100 nm polycarbonate membrane (Millipore) using a mini-extruder device. The resulting suspension, designated as CDNVs1, was stored at 4°C for subsequent experiments

1.2.2 Sucrose density gradient ultracentrifugation (CDNVs2)

The clarified sap was carefully layered onto a sucrose density gradient consisting of 8%, 30%, 45%, and 60% w/v sucrose solutions and subjected to ultracentrifuged at $100,000 \times g$ for 2 h at 4°C . The vesicle-enriched fraction collected from the interface layer between the 30% and 45% sucrose layers was diluted in PBS and concentrated using a 100 kDa molecular weight cutoff ultrafiltration device. The concentrate was then extruded five times through a 100 nm polycarbonate membrane to obtain the CDNVs2 suspension.

1.2.3 PEG precipitation

The clarified plant sap was mixed with PEG 8000 solutions at varying final concentrations (5%, 10%, and 20% w/v) by combining equal volumes of sap and PEG 8000 solutions. The mixtures were incubated at 4°C for 12 h to promote vesicle

precipitation. The resulting precipitates were collected by centrifugation at 10,000 $\times g$ for 30 min at 4°C, resuspended in PBS, and subjected to five successive extrusions through a 100 nm polycarbonate membrane. The final preparations, designated as CDNVs3-2.5%, CDNVs3-5%, and CDNVs3-10%, were stored at 4°C for further use.

1.3 Lipidomic profiling

Lipid composition analysis of CDNVs was performed by Beijing Bio-Tech Pack Technology Co., Ltd. using ultra-high performance liquid chromatography-tandem mass spectrometry (UHPLC-MS/MS). Lipids were extracted via methyl-tert-butyl ether (MTBE) method and separated on an ACQUITY UPLC BEH C18 column (1.7 μm , 2.1 \times 100 mm; Waters, USA) with a mobile phase consisting of acetonitrile-isopropanol (60:40, v/v) containing 10 mM ammonium formate. Mass spectrometric detection was carried out on a TripleTOF 6600 system (SCIEX, USA) operating in both positive and negative electrospray ionization modes over a mass range of m/z 200–1200. Relative lipid abundances were quantified using internal standards (d7-cholesterol and C17:0 lysophosphatidylcholine) and expressed as percentages of total lipid signals.

2. Supplemental Table and Figure legends:

Table S1. Primer sequences

Figure S1. Characterization of CDNVs. (A) Representative images of CDNVs isolated through ultrafiltration (CDNVs1), ultracentrifugation (CDNVs2), and PEG precipitation (CDNVs3). (B) Quantitative comparison of CDNVs yields across the three isolation methodologies. (C) Particle concentration and size distribution of CDNVs, analyzed by NTA. (D) Particle number-to-microgram protein ratio of CDNVs. (E) Assessment of DPPH radical scavenging efficacy.

Figure S2. Lipidomic profile.

Figure S3. Stability evaluation of CHOL@CDNVs. Representative visual image of cholesterol-modified CDNVs and cholesterol-deficient CDNVs following 4-weeks storage at 4 °C.

Figure S4. Cytotoxicity assay. Determination of optimal endocytosis inhibitor

concentrations.

Figure S5. Quantitative analysis of intracellular ROS via DCF fluorescence. Single-cell quantification of DCF mean fluorescence intensity (MFI) was performed using ImageJ software. $p < 0.05$, $*p < 0.01$, $**p < 0.001$.

Figure S6. Serum levels of ALT (A) and AST (B) in all experimental groups after treatment.

Table S1

Gene	Primer
<i>GAPDH</i> Forward	AGGAGCGAGACCCCCTAAACA
<i>GAPDH</i> Reverse	AGGGGGGCTAAGCAGTTGGT
<i>IL-1β</i> Forward	TGCCACCTTTGACAGTGATG
<i>IL-1β</i> Reverse	TGATACTGCCTGCCTGAAGC
<i>TNF-α</i> Forward	GGCAGGTCTACTTGGAGTCATTGC
<i>TNF-α</i> Reverse	ACATTGAGGCTCCAGTGAATTGG
<i>IL-6</i> Forward	TTGGTCCTAGCCACTCCTTC
<i>IL-6</i> Reverse	TGGAGTCCAGCAGACTCAAT
<i>IL-10</i> Forward	TTTCACAGGGAGAAATCG
<i>IL-10</i> Reverse	CCAAGCCTTATCGGAAATGA
<i>iNos</i> Forward	AGCACAGAATGTTCCAGAATCCC
<i>iNos</i> Reverse	GTGAAATCCGATGTGGCCTTG
<i>Arg-1</i> Forward	GGAAGACAGCAGAGGAGGTGAA
<i>Arg-1</i> Reverse	GGTAGTCAGTCCCTGGCTATGG

Figure S1

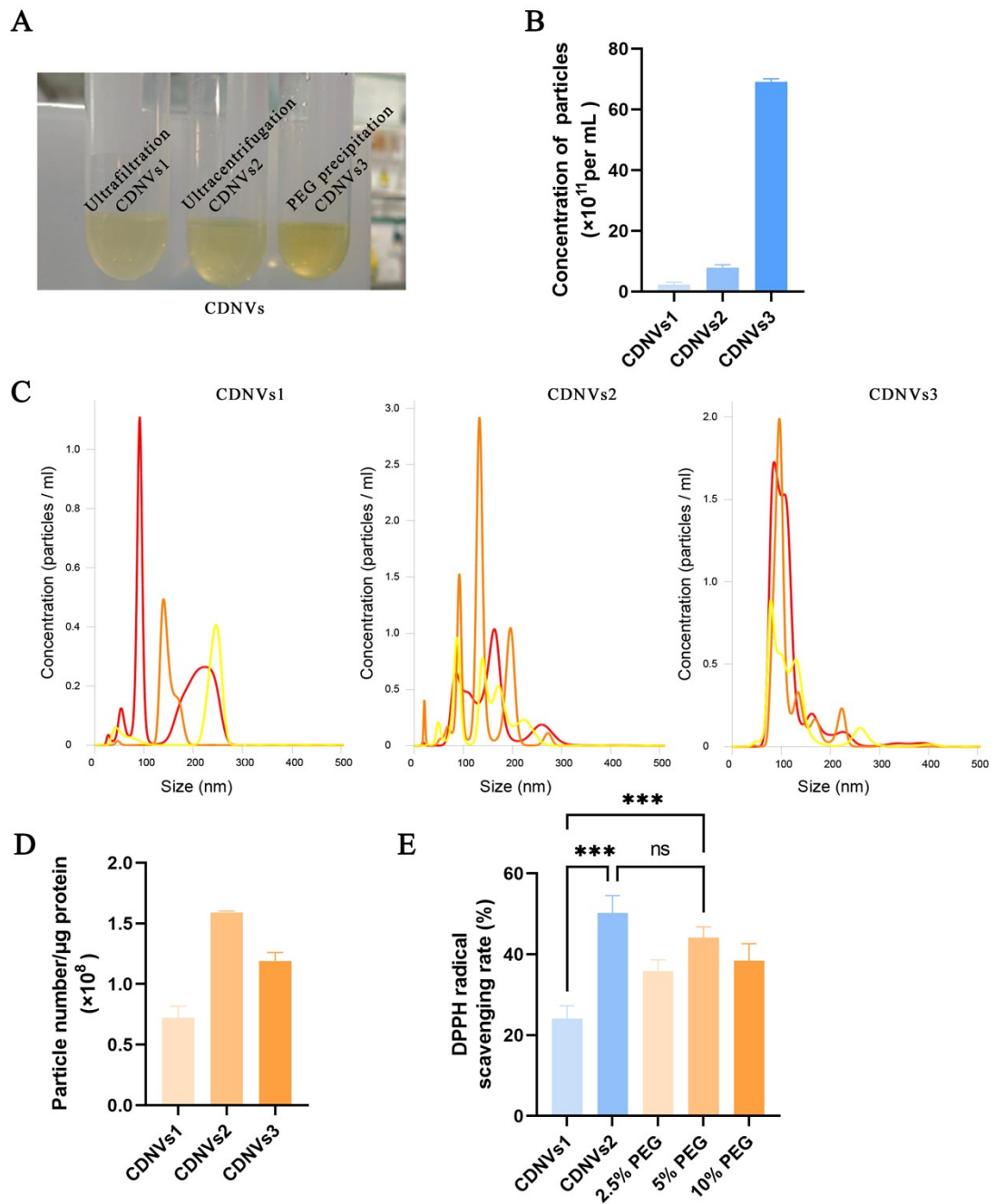


Figure S2

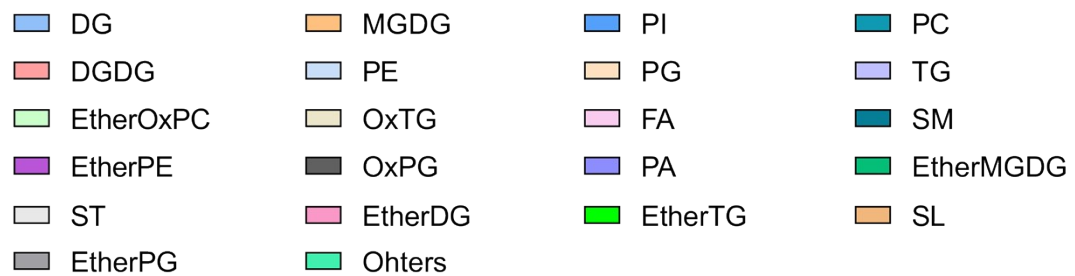


Figure S3



Figure S4

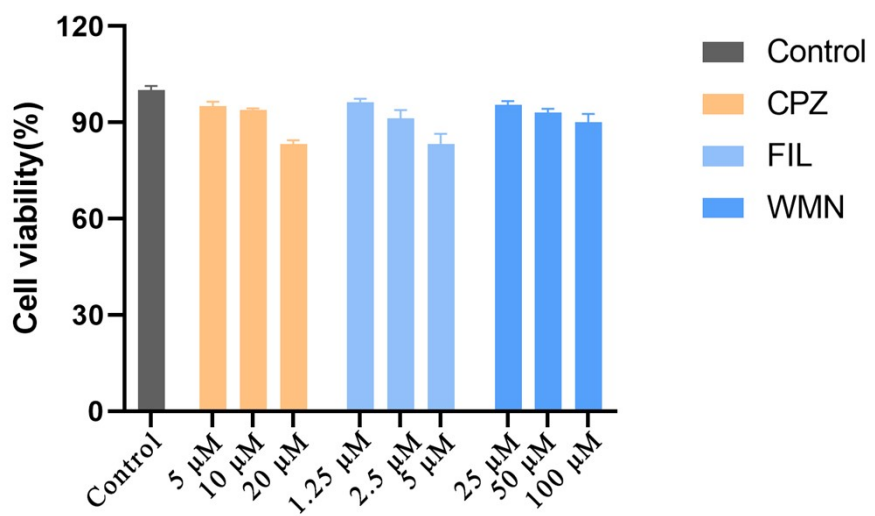


Figure S5

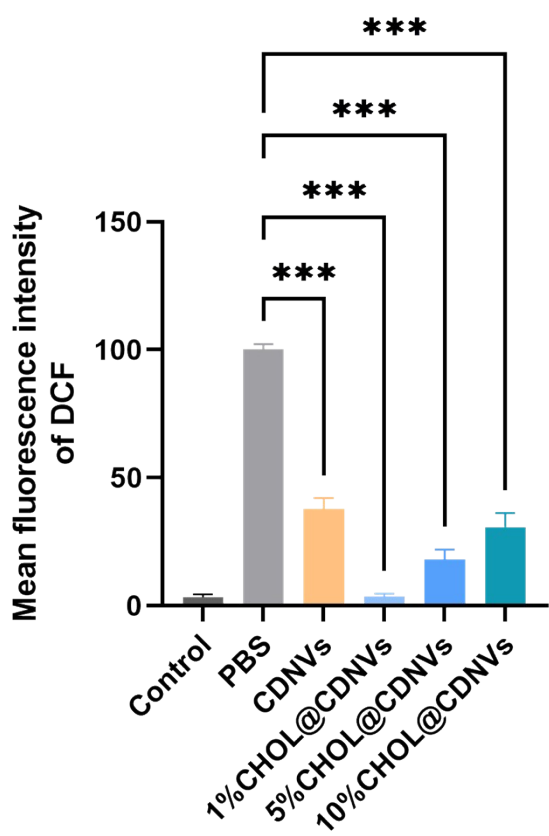


Figure S6

